

Supplement of Atmos. Chem. Phys. Discuss., 14, 23949–23994, 2014
<http://www.atmos-chem-phys-discuss.net/14/23949/2014/>
doi:10.5194/acpd-14-23949-2014-supplement
© Author(s) 2014. CC Attribution 3.0 License.



Supplement of

Meteorological controls on the vertical distribution of bromine monoxide in the lower troposphere

P. K. Peterson et al.

Correspondence to: W. R. Simpson (wrsimpson@alaska.edu)

2.4 Reduction of the Full Profile

Figures S1 and S2 show the remainder of the timeseries shown in Fig. 4 of the manuscript.

2.5 Other Fieldsites

5 The CIMS sampling inlet used was nearly identical to that described by Liao et al. (2011). The outer portion of the inlet was a 4.6 cm ID aluminum pipe that extended ≈ 9 cm beyond the wall of the sampling building. A blower was used to pull a total flow of ≈ 300 lpm through 33 cm of the aluminum pipe. 7.4 lpm of this flow was sampled into a 30°C heated 25 cm, 0.65 cm ID PFA path that included a custom three-way valve for calibration and background measurements. Following the valve, 2.0 lpm entered the CIMS flow reactor through a 0.51 mm diameter orifice. $\text{I} \cdot (\text{H}_2\text{O})_n^-$ was produced in the flow reactor by passing 1.7 lpm of 5 ppm methyl iodide (CH_3I) in N_2 through a ^{210}Po ionizer with water addition in N_2 (0.12 lpm) from a room temperature ($\approx 20^\circ\text{C}$) 1 L bubbler to the flow reactor, which was held at a constant pressure of 13 Torr. The primary difference between the CIMS instrument used by Liao et al. (2011) and that used herein is that two 77 l/s turbomolecular pumps are utilized on the vacuum region instead of two 250 ls^{-1} pumps. In addition, the quadrupole mass analyzer has a 9 mm o.d. compared to 18 mm (Liao et al., 2011).

15 Ambient CIMS measurements were interrupted for other experiments, as well as backgrounds and calibrations. Glass wool, used for the background scrubber, has been shown to remove halogen species at $> 95\%$ efficiency (Neuman et al., 2010; Liao et al., 2012). CIMS sensitivity to Br_2 varied through the BROMEX study depending on H_2O addition and detector sensitivity. Correspondingly, 20 BrO sensitivity (at mass 224) ranged from 2-16 Hz per ppt. To account for this changing sensitivity, the signals were normalized to the reagent ion at mass 147 ($\text{I} \cdot (\text{H}_2^{18}\text{O})^-$). The normalized calibration Br_2 calibration factor, defined as $\text{mass } 287 / ([\text{Br}_2] \cdot \text{mass } 147)$ was 0.00270 (± 0.00008) $\text{Hz Hz}^{-1} \text{ mol pmol}^{-1}$. A relative sensitivity of BrO (mass 224) relative to Br_2 (mass 287) of 0.47 was utilized for BrO calibration Liao et al. (2011).

25 References

- Liao, J., Sihler, H., Huey, L. G., Neuman, J. A., Tanner, D. J., Friess, U., Platt, U., Flocke, F. M., Orlando, J. J., Shepson, P. B., Beine, H. J., Weinheimer, A. J., Sjostedt, S. J., Nowak, J. B., Knapp, D. J., Staebler, R. M., Zheng, W., Sander, R., Hall, S. R., and Ullmann, K.: A comparison of Arctic BrO measurements by chemical ionization mass spectrometry and long path-differential optical absorption spectroscopy, *Journal of Geophysical Research*, 116, 1–14, doi:10.1029/2010JD014788, <http://www.agu.org/pubs/crossref/2011/2010JD014788.shtml>, 2011.
- Liao, J., Huey, L. G., Tanner, D. J., Flocke, F. M., Orlando, J. J., Neuman, J. A., Nowak, J. B., Weinheimer, A. J., Hall, S. R., Smith, J. N., Fried, A., Staebler, R. M., Wang, Y., Koo, J.-H., Cantrell, C. A., Weibring, P., Walega, J., Knapp, D. J., Shepson, P. B., and Stephens, C. R.: Observations of inorganic bromine (HOBr, BrO, and Br₂) speciation at Barrow, Alaska, in spring 2009, *Journal of Geophysical Research*, 117, D00R16, doi:10.1029/2011JD016641, <http://doi.wiley.com/10.1029/2011JD016641>, 2012.
- Neuman, J. a., Nowak, J. B., Huey, L. G., Burkholder, J. B., Dibb, J. E., Holloway, J. S., Liao, J., Peischl, J., Roberts, J. M., Ryerson, T. B., Scheuer, E., Stark, H., Stickel, R. E., Tanner, D. J., and Weinheimer, a.: Bromine measurements in ozone depleted air over the Arctic Ocean, *Atmospheric Chemistry and Physics*, 10, 6503–6514, doi:10.5194/acp-10-6503-2010, <http://www.atmos-chem-phys.net/10/6503/2010/>, 2010.

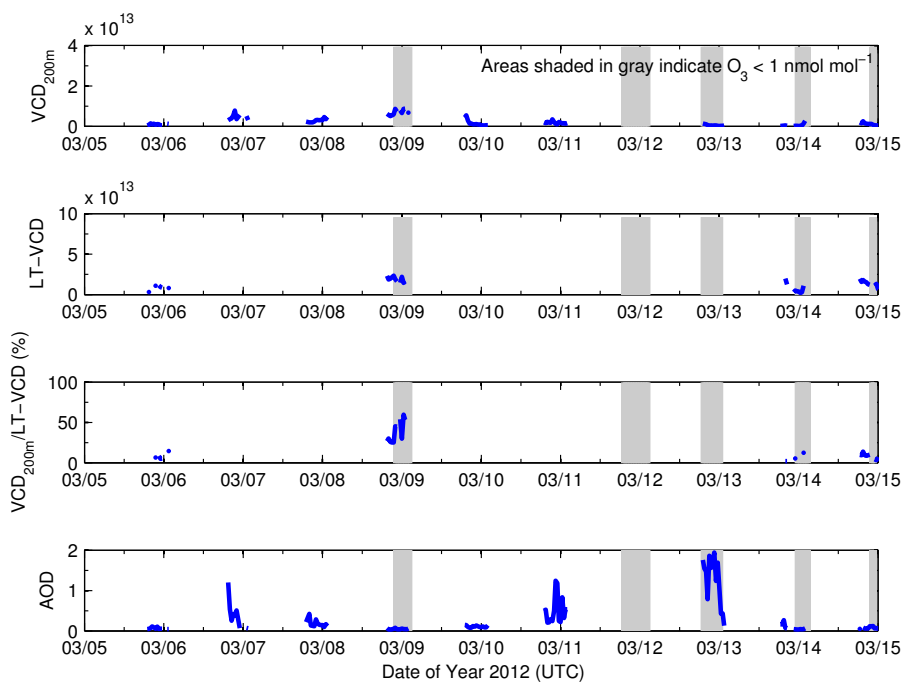


Figure S1. A portion of the timeseries of BrO observed during this study. The top panel represents the VCD_{200} , the second panel represents the $LT-VCD$, both of which have units of molecules cm^{-2} . The third panel shows the percentage of the $LT-VCD$ observed in the lowest 200m, while the bottom panel shows the aerosol optical depth over the course of this study. In the third panel, ratios are not calculated for events that have a $LT-VCD$ below 5×10^{12} molecules cm^{-2} . Shaded areas represent potentially titrated air masses near the surface ($O_3 < 1 \text{ nmol/mol}$).

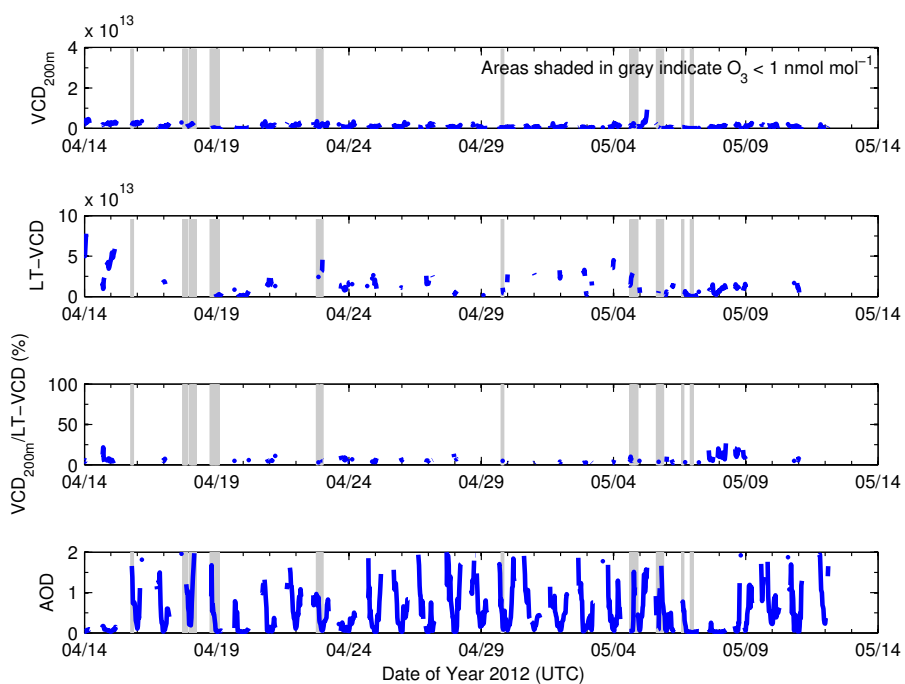


Figure S2. A portion of the timeseries of BrO observed during this study. The top panel represents the VCD_{200} , the second panel represents the LT-VCD, both of which have units of molecules cm^{-2} . The third panel shows the percentage of the LT-VCD observed in the lowest 200m, while the bottom panel shows the aerosol optical depth over the course of this study. In the third panel, ratios are not calculated for events that have a LT-VCD below 5×10^{12} molecules cm^{-2} . Shaded areas represent potentially titrated air masses near the surface (Ozone < 1 nmol/mol).